Internal Tide Generation Over a Continental Shelf: Analytical and Numerical Calculations

Gaëlle Faivre

Final report of the 2nd year engineering degree at the MATMECA School

Advisors
Pr. Eric Chassignet, Flavien Gouillon and Alexandra Bozec

September 2008

Acknowledgment

I thank Eric Chassignet for given me the opportunity to do this internship at the Center for Ocean-Atmospheric Prediction Studies (COAPS).

I have discovered a very interesting science field, learning the basics in oceanography and ocean modeling, extending my knowledge in computer programming such as SHELL, MATLAB and IDL. I also improved my technical and relational English.

I thank Flavien Gouillon and Alexandra Bozec too, for having supervised me during my internship and for their contribution to improve my skills and learning. I also thank Dr. Stephen Griffith for his help on the analytical solution part and providing some codes for the analytical solution.

Finally, I would like to thank Austin Todd, Meredith Field, Dmitri Dukhovskoy and Jordan Yao for giving me several rides from home to work, and all the COAPSians for their kindness and their warm welcoming, and especially, Marie Boisserie and Steve Morey.

Contents

I. Motivation

To complete my second year in MATMECA, Engineering school, I did my internship at the Center for Ocean-Atmospheric Predictions Studies (COAPS, Florida State University) from June to September 2008, in Tallahassee, the state capital of Florida, USA.

COAPS performs research in air-sea interaction, ocean and coupled air-sea modeling, climate prediction, statistical studies, and predictions of social/economic consequences due to ocean-atmospheric variations. Students in COAPS come from a wide variety of departments including meteorology, mathematics, computer science, and physical oceanography. COAPS has provided the perfect opportunity for me to complete an internship and a science project, being captivated by the oceanic and atmospheric phenomena.

When ocean tidal currents encounter undersea topography, waves called internal tides are generated. Internal waves are ubiquitous in stratified aquatic environments. These waves propagate into the ocean interior and can contribute significantly to the oceanic mixing and the large-scale circulation when they break (*Munk and Wunsch*, 1998), influencing how energy is transported throughout the ocean. Recently, a numerical study by *Simmons et al* [2006], showed that the global ocean circulation is very sensitive to this tidally driven mixing. However, many open issues still remain on the mixing induced by the internal wave breaking process.

The generation and propagation properties of the internal wave are sensitive to subtle variations of the ocean stratification, tidal forcing amplitude, and topography, especially on rough topography (i.e. oceanic ridges, trenches, seamount, continental shelves, etc…). At such locations, the dynamic of an internal wave can be strongly non-hydrostatic and thus cannot be well-resolved in Oceanic General Circulation Models (OGCMs) that usually make the hydrostatic approximation. This study aims towards a better understanding of how internal wave are generated particularly at a continental shelf, which is considered as a very rough topography in the ocean. In order to do so, numerical experiments are conducted using the HYbrid Coordinate Ocean Model (HYCOM).

The internal waves generated at a continental shelf affects a wide variety of other domains such as local ecosystems (by distributing and transporting nutrients), sediment transport, oil production companies, and submarines navigation.

First, I present a brief review on the equation of motion that described the oceanic and atmospheric circulation with a particular interest on the internal wave theory. In a third section, I present analytical and numerical calculations of internal wave generation over a continental shelf. Results and discussion are presented in a fourth section.

II. Theoretical Background

a. Description of the Navier-Stokes equation

The geophysical fluid dynamics is the study of naturally occurring oceanic and atmospheric flows. Without its atmosphere and oceans, our planet will not be able to sustain life. Seventy percent of the Earth's surface is covered by the ocean. Conditions at the sea have influenced human activities like exploration, commerce, fisheries and wars.

All of us, scientists, engineers, and the public are becoming increasingly concerned about the dispersion of pollutants in the environment like, and especially about their cumulative effect. When the accumulations of greenhouse gases in the atmosphere will lead to global climatic changes? What are the various roles played by the oceans in maintaining our present climate? These questions could be partly answered by a better understanding of atmospheric and oceanic dynamics, through the use of observational datasets and numerical models. For example, geophysical fluid dynamics helps us predict the paths of hurricanes, which allow us to save many human lives.

The most important equation in geophysical fluids dynamics that describe flow motion is the Navier-Stokes equation given by (1).

$$\underbrace{\frac{\partial \vec{U}}{\partial t} + \vec{U} \bullet \nabla \vec{U}}_{1} + \underbrace{2\vec{\Omega} \times \vec{U}}_{2} = \frac{1}{\rho}\left(\underbrace{-\nabla p}_{3} + \underbrace{\vec{F}_v}_{4} + \underbrace{\mu \Delta \vec{U}}_{5}\right) \qquad (1)$$

Where: 1 is the acceleration of a water parcel

2 is Coriolis force

3 is the pressure gradient term

4 are the voluminal forces

5 are the viscous forces

The water parcel acceleration (term 1) is defined by an unsteady acceleration plus a non linear term, the convective acceleration. In an incompressible flow, the term $\vec{U} \bullet \nabla \vec{U}$ equals 0. Some forces act upon the water parcel such as the Coriolis force (term 2) which depends on the velocity of the moving fluid and the angular velocity (due to the rotation of the Earth). The right hand side of the equation is a summation of the pressure gradient (term 3), the body forces such as the tides, the atmospheric forcing $\vec{F}_v$ (term 4) and conventionally $\mu \Delta \vec{U}$ (term 5) describes viscous forces and for incompressible flow, this is only a shear effect.

b. Internal wave theory

Internal waves occur in stably stratified fluids when a water parcel is displaced by some external force and is restored by buoyancy forces. Then the restoration motion may overshoot the equilibrium position and set up an oscillation thereby forming an internal wave that will propagate. Figure 1 shows observed internal waves generated at the Strait of Gibraltar. They have been studied by several groups of researchers in geophysical fluid dynamics, acoustics ocean optics, sediment transport, plankton advection and vertical mixing.

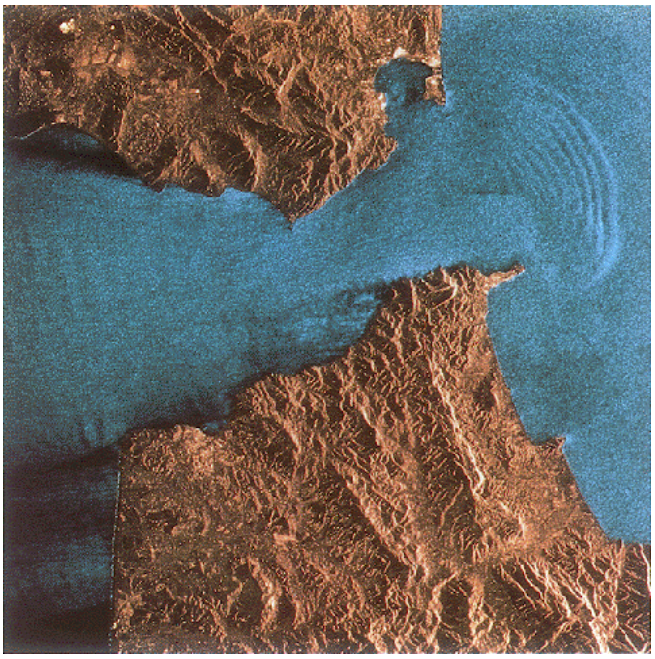

Figure 1: Example of surface signature of internal waves (wavelength about 2 km) which seem to move from the Atlantic Ocean to the Mediterranean Sea, at the east of Gibraltar and Ceuta.

Usually, internal waves have much lower frequencies and higher amplitudes than the surface gravity waves because the density differences within fluid are generally smaller than the density of the fluid itself. The typical horizontal length scale of internal waves is of the order 1 to 100 km.

A classic paper by *Munk and Wunsch* [1998] showed that the dissipation of these waves by turbulence could be responsible for half of the energy to mix the ocean and maintain the strength of the meridional overturning circulation. Thus, knowledge of the internal wave breaking process is key to understanding the global climate system.

Packets of nonlinear internal waves have been observed throughout the world, primarily on continental shelves. One important internal wave generation mechanism comes from the interaction between rough topography and the semi-diurnal barotropic tide. Thus, these waves are generated with a tidal period of 12.421 hour period. Their time scale of their propagation is from minutes to days with a horizontal velocity of 0.05 $m.s^{-1}$ to 0.5 $m.s^{-1}$.

In a non-rotating environment, the internal wave dispersion relation for a uniformly stratified fluid is governed by:

$$\frac{\partial^2}{\partial t^2}\left(\frac{\partial^2 w}{\partial x^2}+\frac{\partial^2 w}{\partial z^2}\right)+N^2\frac{\partial^2 w}{\partial x^2}=0 \quad (2)$$

The general solution has the following form: $w = A\exp(ikx + imz - i\omega t)$ (3)

Where x and z are respectively the horizontal and vertical coordinate, N is the buoyancy frequency, w is the vertical velocity, A is a constant, k and m are respectively the horizontal and vertical wave numbers, ω the tidal frequency, t the time.

The tidal frequency has the following form: $\omega^2 = \left(f^2m^2 + N^2k^2\right)/\left(k^2 + m^2\right)$ (4)

From (2), we can clearly see that the propagation of an internal wave depends only on the tidal forcing frequency, on its geographic latitude and on how the water changes density with depth.

III. Analytical solution of internal wave generation over a continental shelf

a. Description of the analytical configuration

In this section, we present the analytical solution of the interaction of an internal wave with an idealized continental shelf described in *Griffiths and Grimshaw* [2007]. We assume that the problem is two-dimensional, that the fluid is divided in two layers of different densities and finally that we have a free surface.

The topography is defined as follow:

$$\begin{cases} h(x) = h_L & for \quad x < x_L \\ h(x) \approx h_L\left(1-\left(1-\frac{h_L}{h_R}\right)\frac{x-x_L}{L_S}\right)^{-1} & for \quad x_L < x < x_R \\ h(x) = h_R & for \quad x > x_R \end{cases} \quad (5)$$

where h_L is the depth on the shelf, h_R is the depth of the deep ocean, x_L and x_R are respectively the abscissa of the shelf break and the deep ocean (See Figure 2). The length of the shelf slope is $L_S = x_R - x_L$ and the length of the shelf is $L_C = x_C$.

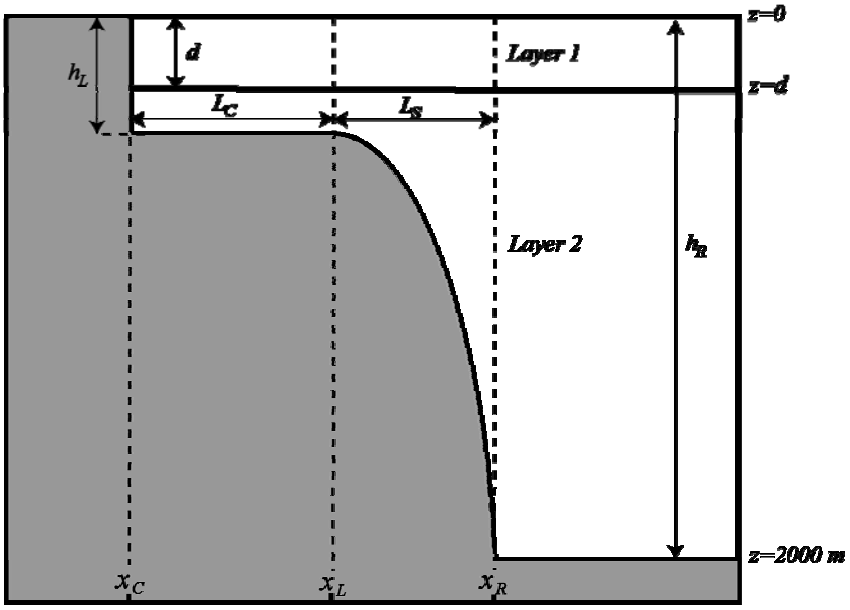

Figure 2: schematic of the analytical model configuration.

b. General solution

The flow is governed by the following equations:

$$\frac{\partial u}{\partial t} = -\frac{1}{\rho_0}\frac{\partial p}{dx} \qquad (6)$$

$$\frac{\partial p}{\partial z} = -g\tilde{\rho} \qquad (7)$$

$$\frac{\partial \rho}{\partial t} + \frac{\partial \rho_0}{\partial z} w = 0 \qquad (8)$$

$$\frac{\partial u}{\partial x} + \frac{\partial w}{dz} = 0 \qquad (9)$$

where u and w are respectively the velocity in the x and z directions

$\tilde{\rho}$ is the density deviation from the density background state (ρ_0)

p is the pressure deviation from the pressure background state

f is the Coriolis parameter

g is the acceleration due to the gravity

The tidally forced baroclinic mode equation is written as:

$$\left(\frac{d^2}{dx^2} + \frac{\omega_f^2}{c_1^2}\right)\hat{U}_1 = -\frac{d^2}{dx^2}\left[\left(\frac{1+(x-x_L)/L_C}{1+L_S/L_C}\right)\frac{c_1^2}{c_\infty^2}\right] \qquad (10)$$

the resulting barotropic zonal velocities are given by:

$$u(x) = \frac{Q}{h(x)}\left(\frac{1+(x-x_L)/L_C}{1+L_S/L_C}\right) \qquad (11)$$

Where Q is the transport, $\hat{U}_1$ is the baroclinic mode 1 forcing, c_1 is the wave speed for the baroclinic mode 1 and is defined as $c_1 = c_\infty\left(1-\frac{d}{h}\right)^{1/2}$ with $c_\infty = \left(\frac{gd\Delta\rho}{\rho_0}\right)^{1/2}$, d representing the depth of the first layer. In order to find an exact solution to this analytical problem, we suppose that c_1 can be rewritten as:

$$c_1 = c_L + (c_R - c_L)(x - x_L)/L_S \quad (12)$$

Griffiths and Grimshaw [2004] have introduced an non-dimensional parameter, s_1, which describes the steepness of the slope: $s_1 = \frac{c_R - c_L}{\omega_f L_S}$, where $\omega_f = \sqrt{\omega^2 - f^2}$.

At the free surface, using the boundary conditions $z = -h(x)$, and $\vec{u} \bullet \vec{n} = 0$, we solve (7-9) and we obtain:

$$w = -u\frac{\partial h}{\partial x} \text{ at } z = -h(x)$$

$$p = g\rho_0(0)\zeta \text{ at } z = 0$$

where ζ represents the linearized vertical particle displacement.

Thus we can also write: $w = \frac{\partial \zeta}{\partial t}$ (13)

For our study, the slope is abrupt, that means $\frac{L_S}{L_C} = 0$ (because $L_S \to 0$), then, we can obtain the interface displacement thanks to the following expression:

$$\zeta(z = -d) = -\zeta_i \left\{ \sin(\omega t) + \frac{1}{2}\sin\left[k(x - x_L) - \omega t\right] - \frac{1}{2}\sin\left[k(x - x_R) + \omega t\right] \right\} \quad (14)$$

Where *k* is the wavenumber defined by $k(x) = \frac{\omega_f}{c_1(x)}$.

For $x_L < x < x_R$, the vertical particle displacement is given by:

$$\zeta_i = 2Qc_L(c_R - c_L)(\omega L_S c_\infty^2)^{-1} \quad (15)$$

The interface displacement can be observed in the schema in the below.

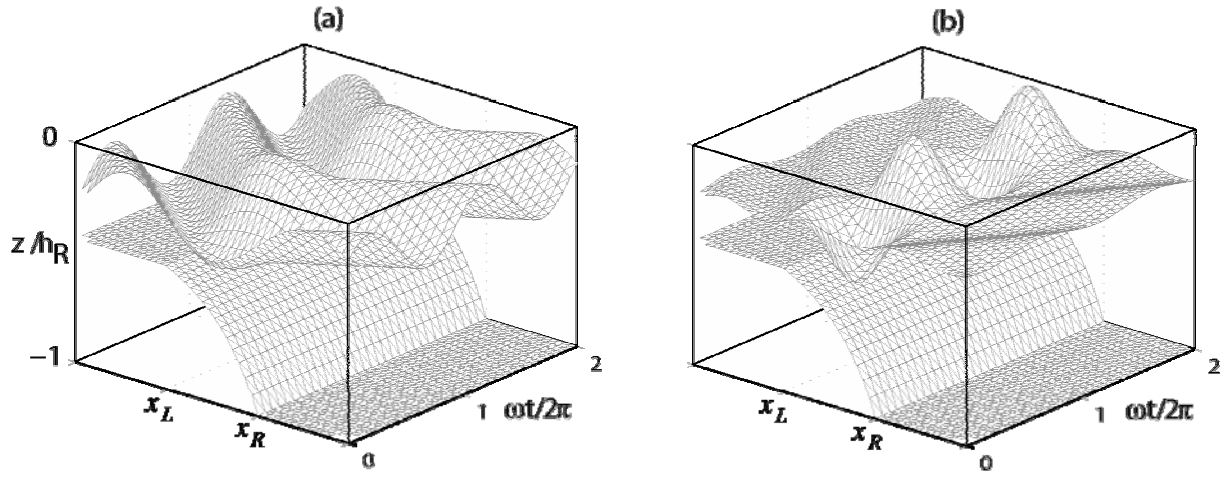

Figure 2: Interface displacement (a) for $s_1 = \log(c_R / c_L)/(\pi)$ and (b) for $s_1 = \log(c_R / c_L)/(2\pi)$, with $c_L / c_R = 0.8, d / h_L = 0.5$

The energy fluxes J_L and J_R are defined at the abscissa x_L and x_R corresponding respectively to the abscissa of the shelf break and the deep ocean. We choose a constant ratio $\frac{c_L}{c_R} \approx 0.7$, and see the dependence of the energy fluxes as a function of the steepness parameter, s_1 (Figure 3). The energy fluxes at the shelf break are given by the expression:

$$J_L = \frac{c_L}{c_R}\left(1-\frac{c_L}{c_R}\right)^2\left(1+\frac{c_R^2}{\omega_f^2}\right) \qquad (16)$$

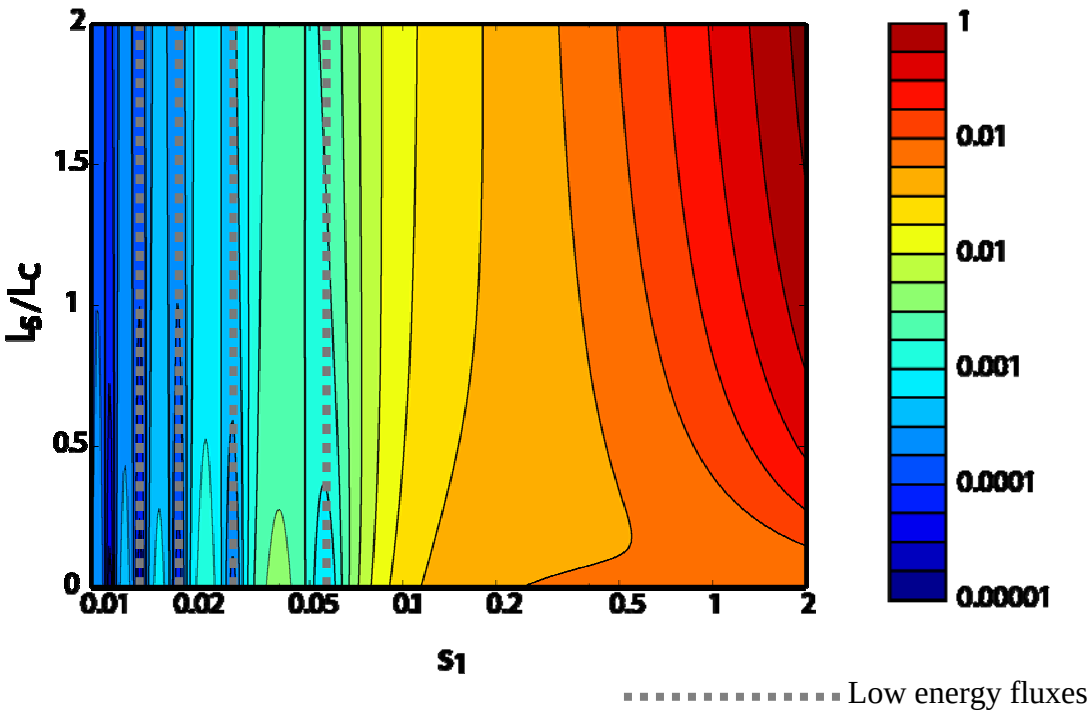

Figure 3: Non-dimensional energy fluxes for the exact two-layer solution at $c_L / c_R = 0.7$, vertical dotted lines represent the low energy fluxes.

Figure 3 shows that as the slope steepness increases, the energy fluxes increase. Indeed, if we pose $\frac{c_L}{c_R} > \frac{1}{3}$, the forcing term in the equation (12) increase monotonically over the entire slope with the ratio $\frac{L_S}{L_C}$. As a result, the energy fluxes given by equation (16) also increase. However, for smaller s_1 ($s_1 < 0.05$), the dominant behavior appears to be related to a more local dynamic. For example, when $s_1 > 0.05$, we notice that J_L increases when $\frac{L_S}{L_C}$ increases, while when $s_1 = 0.015$, J_L and J_R decrease when $\frac{L_S}{L_C}$ increases.

In addition to these results, Figure 3 shows low energy fluxes for particular values of s_1. These low energy fluxes are predicted across the slope as a function of the change in phase (vertical gray dashed lines), namely $\Delta\theta$ defined as:

$$\Delta\theta = \int_{x_L}^{x_R} k(x)dx = \frac{1}{s_1}\log\frac{c_R}{c_L} \qquad (17)$$

where $k(x) = \frac{\omega_f}{c_1(x)}$ is the wave number when we assume that the phase of the internal mode varies rapidly compare with the slope. Indeed, low values of J_L are observed when $\Delta\theta = 2n\pi$, with *n*=1,2,3,4 for the first four predictions. On the contrary, when $\Delta\theta = (2n-1)\pi$, there is strong wave propagation away from the slope and the resulting energy flux J_L is high.

The physical explanation is: when $\Delta\theta = 2n\pi$, the waves reach the slope after completing a full period. However, waves with phase $\Delta\theta = (2n-1)\pi$ break on the slope before finishing a full cycle of oscillation and thus generate a lot of energy. There is also a direct interplay between the energy fluxes and the vertical interface displacement. As Figure 2 shows us, for $s_1 = \log(c_R / c_L)/(2\pi)$, internal waves are more located at the shelf break. However, for $s_1 = \log(c_R / c_L)/\pi$, they are more spread on the coastline and the deep ocean.

We will now conduct several numerical simulations with HYCOM to evaluate the model for the same configuration and parameters as in the analytical solution.

IV. Comparison of numerical simulations against analytical solutions

Ocean models can provide an experimental apparatus for the scientific rationalization of ocean phenomena, and allow us to have a better understanding and prediction of aspects of the ocean. Different kind of numerical models are used for large-scale studies (global models) as well as small scale studies (high resolution near coastal area), and from few days processing (tides) to centuries (ocean current).

One way to sort out the different models is by their respective approach of vertical coordinate treatments:

- The *z*-coordinate models, traditionally used in global ocean climate models, divide the water column in fixed level from the surface (*z=0*) to the bottom of the topography (*z=-H*).

- Terrain-following-coordinate models, generally used for the coastal applications, use fixed levels defined as:

$$\sigma = \frac{z - \zeta}{H + \zeta}$$

Where $\zeta(x, y, t)$ is the displacement of the ocean surface from its resting position *z=0* and *z=-H(x,y)* the bottom topography.

- The last ones are the isopycnal coordinate (ρ-coordinate) models referenced to a given pressure. These models are inherently adiabatic and accept arbitrarily steeply sloped topography.

A main disadvantage in *z*- and σ-coordinate models is the apparition of a spurious diapycnal mixing due to the numerical advection schemes that can not maintain adiabatic properties of a water parcel. The σ–coordinate models also have gradient error computation at steep slope. Also, all of these models is that they use a single coordinate type to represent the water column but not a single one can by itself be optimal everywhere in the ocean. This is why many developers have been motivated to pursue research into hybrid approaches, which is the subject of the following subsection.

a. The Hybrid Coordinate Ocean Model (HYCOM)

The HYbrid Coordinate Ocean Model (HYCOM) is the result of collaborative efforts among the University of Miami, the Naval Research Laboratory (NRL) and the Los Alamos National Laboratory (LANL) and combines all the three vertical discretization seen in the previous section. For HYCOM, this vertical coordinate system is showed Figure 4.

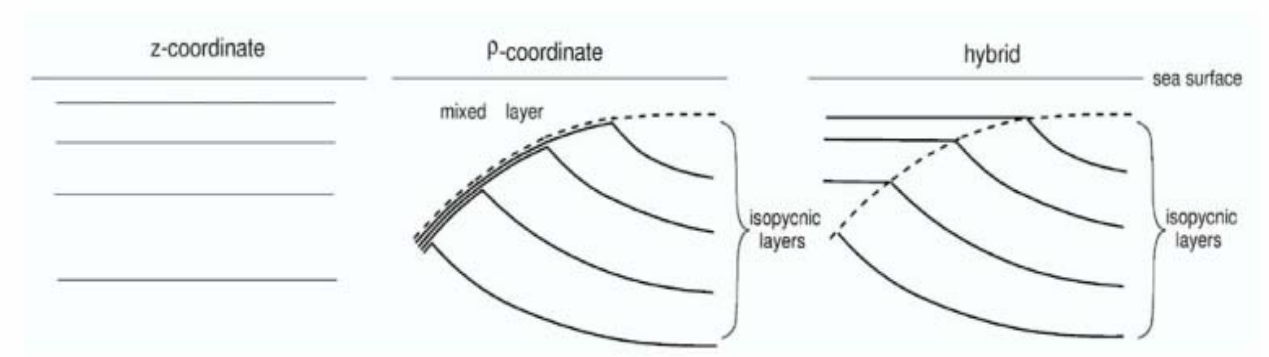

Figure 4: Description of the *z*-, ρ-, and hybrid coordinates of HYCOM.

HYCOM behaves like a conventional sigma model in very shallow and/or unstratified oceanic regions, like a *z*-level coordinate model in the mixed layer or other unstratified regions, and like an isopycnic-coordinate model in stratified regions. In doing so, the model combines the advantages of the different types of coordinates in optimally simulating coastal and open-ocean circulation features. In our study, HYCOM is run in a fully isopycnal mode to have a controlled diapycnal mixing.

b. Model configuration

For this study, we use the version 2.2 of HYCOM, on a rectangular basin configuration with 312m horizontal resolution, 2 isopycnal layers (layer 1 and 2 of potential density 24.77 kg.m^{-3} and 26.40 kg.m^{-3} respectively), no bottom friction to isolate the tidal energy conversion, closed east and west boundaries. The model is forced with a barotropic tide of varying frequency [2.229x10^{-6} s^{-1}, 3.3435 x10^{-4} s^{-1}] at the eastern boundary and we impose a constant ratio $\frac{c_L}{c_R} = 0.745$. Outputs are saved every hour to avoid tidal aliasing. The model reaches a stable energy state after a day and a half and energetic computations are made between 6 and 10 tidal cycles. The topography is defined by equation (5) with the particular values: h_L=200m, h_R=2000m, x_L = 100km, and x_R= 200km, thus L_s=100km.

c. Results

We compute the energy fluxes at the shelf break (x_L) for each simulation and plot them as a function of the steepness parameter (Figure 5). In order to compare to the analytical solution we compute the low energy phases and find for which value of the steepness parameter we should have low energy fluxes. The baroclinic energy fluxes are computed using equation (16).

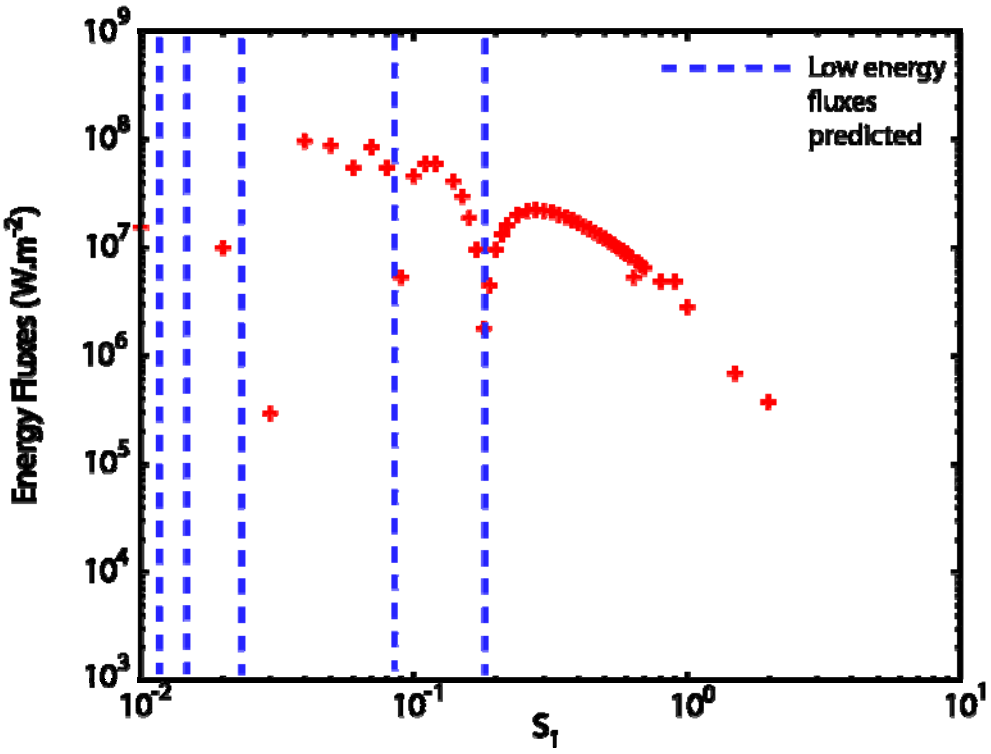

Figure 5: Depth integrated energy fluxes (red crosses) averaged over 1 tidal cycle at x_L as a function of the steepness parameter (s_1) for $h_L / h_R = 0.1$ and $L_S / L_C = 1$ for each simulation. Vertical blue dashed line represents the expected low energy fluxes ($\Delta\theta = 2n\pi$).

We can see high-energy regime in the vicinity of small s_1. However, for s_1 >0.2, the energy strongly decreases. For some specific values of s_1 (0.09, 0.2) it appears that there is a drop in the energy fluxes, these low energy phases well correlate with the predicted one (Figure 5). The energy fluxes are in the order of 1×10^7 W.m^{-2} which is a common energy magnitude for this type of problem (*Venayagamoorthy*, 2006; *Hibiya*, 2004).

V. Discussion

It seems that HYCOM is well representing the energetic of the internal wave since the locations of the low energy fluxes are well correlated to the analytical solution. There are, however, few differences from the theory, mainly that the location of the low energy fluxes is shifted. We try to discuss these issues in this section.

In order to have our interested range of value of s_1 we have varied the tidal frequency forcing between very high (2.229×10^{-6} s^{-1}) and low frequency (3.3435×10^{-4} s^{-1}). Since we are saving the output only every hour, an aliasing in the sampling could lead to errors for small s_1. This problem could be easily resolved by running again the experiment and saving the output with a much higher frequency. The problem could also arise from the numerical model itself. Indeed, HYCOM could slightly have an error on representing the wave speed and/or wavelength. This will lead to a shift in the location of the low energy fluxes, an example would be at s_1=0.02.

The analytical solution only takes into account one baroclinic mode while the model is in fact resolving two. Indeed, HYCOM was run with 3 layers for technical purposes with 2 layers with almost equal density (the density gradient between the two is of the order 10^{-4}). This issue could be resolved by having an analytical solution that considers a 'real' stratification with a full layered ocean.

When we consider higher value of the steepness parameter it seems that the energy slowly decreases. This is a direct influence of the depth of the shelf compare to the depth of the deep ocean as well as the coastline effect. This ratio is constant for us ($h_L / h_R = 0.1$) and has a direct impact on controlling the propagation shoreward or oceanward. The smaller the ratio is the fastest this decrease on the energy fluxes arises. For example, if $h_L / h_R = 0.5$ then the decrease will occur at s_1= 0.9 (*Griffiths and Grimshaw*, 2007). This is coming from the fact that the barotropic forcing decreases as the length of the shelf slope increases (see equation (11) for more details).

This study shows that with few numerical experiments conducted, HYCOM seems to represent well the behavior of strong internal wave (in a supercritical regime). However, a significant drawback is the sparse sampling. With more time, new configurations should be conducted in order to have a full view of the energy fluxes pattern as a function of the steepness parameter. The main improvement would also be to have a more realistic view of this problem and thus extend the problem to a full layered ocean.

VI. Conclusions

In this study we have conducted idealized numerical simulations of internal wave generation over a continental shelf in a 2-layers ocean with HYCOM. We compare the results to the analytical solution derived by *Griffiths and Grimshaw* [2007]. The results are promising since internal wave low energy fluxes seem to be well represented in the model. We believe that HYCOM is very successful on representing the generation and propagation of the internal wave at abrupt slope. The observed shifts in these locations could arise from an aliasing problem, from a lack of numerical experiment, as well as the model itself that could slightly misrepresent the internal wave propagation (wavelength, wave speed). This study would benefit from further development such as providing a real stratification as well as adding more numerical simulations.

References

Griffiths, S. D., Grimshaw, R. H. J., 2007, Internal tide generation at the continental shelf modeled using a modal decomposition: two-dimensional results. *Journal of Physical Oceanography*.

Hibiya, T., 2004, Internal wave generation by tidal flow over a continental slope. *Journal of Oceanography*, Vol **60**, pp. 637-643.

Munk, W., Wunsch C., 1998, Abyssal recipes-II: Energetics of tidal and wind mixing. *Deep-Sea Res.*, **45**, 1977-2010

Simmons, H., Jayne, S., St Laurent, L., Weaver, A., 2003, Tidally driven mixing in a numerical model of the ocean general circulation. *Ocean Modeling* **6**, 245-263.

Venayagamoorthy, S. K., Fringer, O. B., 2006, Numerical simulations of the interaction of internal waves with a shelf break. *Physics of Fluids*, **18**, 076603-1.